Aspartate aminotransferase is required for *Salmonella* expansion in the inflamed gut via TCA anaplerosis

Shealy NG[1], Baltagulov M[1], Avalos HF[1], Olivas J[1], Jones KM[1], Byndloss MX[1,2,3,4]

[1]Department of Pathology, Microbiology, and Immunology, Vanderbilt University Medical Center, Nashville, TN 37232, U.S.A.

[2]Howard Hughes Medical Institute, Vanderbilt University Medical Center, Nashville, TN 37232, U.S.A.

[3]Vanderbilt Institute of Infection, Immunology, and Inflammation, Vanderbilt University Medical Center, Nashville, TN 37232, U.S.A.

[4]Vanderbilt Microbiome Innovation Center, Vanderbilt University, Nashville, TN 37232, U.S.A.

[*] Lead correspondence: mariana.x.byndloss@vumc.org

ABSTRACT

Aspartate represents an important proteogenic amino acid in all living organisms. Many microorganisms can produce aspartate through various biosynthetic processes, utilizing it for energy production and as a precursor for synthesizing other biomolecules, such as amino acids and nucleotides. The enteric pathogen *Salmonella* Typhimurium (*S.* Tm) has developed mechanisms to access aspartate as a nutrient source during expansion in the inflamed gut. However, how *S.* Tm deals with aspartate starvation during infection remains unknown. To address this knowledge gap, we interrogated *Salmonella*'s reliance on the bi-directional aspartate aminotransferase encoded by *aspC* for growth *in vitro* and during host colonization using murine models of *Salmonella* infection. AspC can interconvert aspartate and the TCA intermediate oxaloacetate and is hypothesized to support *S.* Tm cellular demands for aspartate during starvation or support refueling of the TCA cycle via oxaloacetate synthesis. Herein, we find that loss of *aspC* results in a gut-specific *S.* Tm colonization defect that increases with the course of infection. Importantly, *aspC* is dispensable for *S.* Tm systemic colonization. Additionally, we report that loss of *aspC* results in a significant growth defect during respiration of inflammation-derived electron acceptors *in vitro*. Interruption of oxidative TCA cycle progression via TCA enzyme deletion or supplementation with TCA intermediates (i.e., oxaloacetate) abrogates the defect demonstrated by Δ*aspC S.* Tm *in vitro.* Thus, suggesting the requirement for AspC to catabolize aspartate and support the TCA cycle during respiration. Altogether, we report that AspC plays a critical role in *S.* Tm pathogenesis in a gut-specific manner during inflammation through supporting energy generation.

Keywords

Salmonella, Gastroenteritis, Aspartate, Pathogenesis

35 **INTRODUCTION**

36 Despite being the primary site of digestion, the mammalian gut represents a region of nutrient scarcity
37 for potential invading enteric pathogens such as *Salmonella enterica* serovar Typhimurium (*S*. Tm)[1–5]. The
38 reason for this scarcity is the occupation of the major nutrient niches by the resident collection of commensal
39 microbes inhabiting the intestines known as the gut microbiota [6–10]. The gut microbiota has been shown to
40 actively reduce the availability of potential nutrients that potential invaders must compete for through direct
41 catabolism and indirect support of host epithelial cell metabolism and nutrient absorption[11–13]. However, how
42 bacterial pathogens adapt to overcome microbiota-protective mechanisms, such as nutrient sequestration,
43 remains to be fully understood.

44 Recent work demonstrates that, in the context of complex microbiota, enteric bacterial pathogens such
45 as *Citrobacter rodentium* and other pathogenic *Enterobacteriaceae* require the expression of amino acid
46 biosynthesis pathways to colonize and expand[3]. Specifically, through a Tn-seq approach comparing germ-free
47 and conventional mice, it has been demonstrated that mutants with insertions in amino acid biosynthesis
48 pathways exhibit a significant fitness defect in conventional mice compared to germ-free mice. Thus, amino acids
49 represent a critical nutrient for which microbial competition exists. Additionally, it is well-documented that bacteria
50 are sensitive to amino acid starvation, which results in the activation of the stringent response. This response is
51 commonly mediated by the SpoT/RelA system, which senses a reduction in amino acid-charged tRNAs, leading
52 to reduced DNA replication, overall metabolism, and the upregulation of biosynthesis pathways. This body of
53 work highlights the importance of the stringent response during gut colonization, as deleting these pathways in
54 *S*. Tm results in a significant fitness defect and reduced virulence[14]. However, which amino acids are required
55 for enteric pathogens in competition with complex microbiota is largely unknown.

56 Our group and others have previously reported that *S.* Tm requires aspartate for expansion in the
57 inflamed gut through aspartate-dependent fumarate respiration via the aspartate ammonia-lyase, AspA [15,16].
58 Specifically, deletion of *aspA* and the C4-dicarboxylic acid transporter encoded by *dcuA*, specific for aspartate
59 import in *S*. Tm, results in a significant expansion defect during murine infection[15,16]. Thus suggesting that
60 aspartate plays a key role in the ability of *S.* Tm to colonize the intestinal lumen during gut inflammation. However,
61 work by Popp *et al*. and Liu *et al*. demonstrates that aspartate biosynthesis also plays a significant role in
62 *Salmonella* replication within macrophages and the maintenance of bacterial replication and cell size via the

63 aspartate aminotransferase encoded by *aspC*[17,18]. Additionally, recent work by Vayena *et al.* through
64 computational metabolic network mapping of *S*. Tm identified the potential for AspC to participate in the synthesis
65 and breakdown of aspartate[19]. However, there is a knowledge gap in how aspartate prototrophy by *S*. Tm, more
66 specifically the necessity of AspC, impacts the pathogen's fitness during intestinal colonization, including during
67 intestinal inflammation when the pathogen relies on anaerobic respiration to outcompete the resident microbiota.
68 Herein, we observe that deletion of the main aspartate aminotransferase AspC in *S.* Tm results in a
69 significant gut-specific defect in pathogen expansion when comparing intragastric and intraperitoneal routes of
70 infection in CBA/J mice. Based on our previous findings that *S*. Tm gastrointestinal infection results in an
71 increased abundance of luminal aspartate[16], we reasoned that the defect of Δ*aspC S.* Tm may not be the result
72 of aspartate starvation but rather of aspartate catabolism. AspC is known to be a bidirectional enzyme capable
73 of degrading aspartate into the TCA intermediate oxaloacetate. Thus, we hypothesized that one possible reason
74 for the expansion defect *in vivo* was the inability of Δ*aspC S.* Tm to fuel anaplerosis of the TCA cycle via
75 oxaloacetate during anaerobic respiration. Specifically, during gut inflammation, the pathogen has increased
76 access to both aspartate and inflammation-derived electron acceptors such as nitrate or tetrathionate, enabling
77 *S.* Tm's oxidative TCA cycle, using oxaloacetate for citrate synthesis. In line with this hypothesis, we find that
78 *aspC*-deficiency results in significant growth and fitness defects only when *S.* Tm is respiring in an aspartate
79 dose-dependent manner[20–22]. Using gene deletions in key TCA enzymes and supplementation of TCA
80 intermediates, we confirm the role of AspC in supporting the central oxidative metabolism of *S.* Tm during
81 anaerobic respiration. Altogether, this study deepens our understanding of the amino acid utilization by *S*. Tm,
82 *in vivo*.
83
84 **RESULTS**
85 Previous reports demonstrate that multi-organ site pathogens, such as *Staphylococcus aureus*, depend
86 on *de novo* aspartate synthesis for survival in murine osteomyelitis models and other organ sites[23]. Transposon
87 insertions in the aspartate aminotransferase of *S. aureus* result in decreased pathogen survival in the
88 osteomyelitis model of disease, as well as in the heart, kidneys, and liver of infected animals. Thus, suggesting
89 the requirement for aspartate production by the pathogen for survival under the nutrient landscape of systemic
90 organs. Another critical human pathogen is *S.* Tm, being one of the four leading causes of foodborne illnesses

91 worldwide[24]. *S*. Tm is an enteric pathogen with disease centering in the cecum of mice[25,26]. However, *S*. Tm can
92 also cause systemic disease by migrating to the liver, through biliary ducts, as well as the spleen through
93 hijacking of dendritic cells and spread through lymphatic vessels[27,28]. Additionally, the liver and spleen are known
94 reservoirs for *Salmonella* replication in murine models of *S*. Tm-induced Typhoid-like disease and humans
95 infected with *S.* Typhi and *S.* ParaTyphi serovars[17,23,29]. Work by Nuccio *et al.* suggests that *aspC* is highly
96 conserved amongst *Salmonella* serovars capable of causing systemic (Typhoid fever) or gastrointestinal disease
97 (gastroenteritis), suggesting that aspartate biosynthesis may be required for *Salmonella* survival in systemic host
98 sites during infection. However, there is a gap in knowledge regarding the dependence of aspartate
99 aminotransferases broadly by the pathogens in different infection-relevant organ sites.

100 To address whether aspartate biosynthesis is required for *S.* Tm survival during systemic infection, we
101 first constructed a *S.* Tm mutant lacking the major aspartate aminotransferase, encoded by *aspC,* and leveraged
102 this strain to perform a competitive infection between wild-type (WT) S. Tm and the isogenic *aspC*-deficient strain
103 (Δ*aspC*) in genetically resistant CBA/J mice. To do so, we infected CBA/J mice intraperitoneally with 10^4 colony-
104 forming units (CFU) of a 1:1 mixture of wild-type S. Tm and *S.* Tm Δ*aspC* (**Fig. 1A**), allowing the mice to carry
105 the infection for three, four, or five-days before euthanasia. We chose these time points to understand if there
106 were any temporal changes to the dependence of *aspC* by *S.* Tm before and after the onset of severe systemic
107 disease. In line with our choice of time points, mice were maintained for five d.p.i. lost significantly more weight
108 compared to those sacrificed at three d.p.i. (**Fig. 1B**). However, we observed no significant competitive
109 advantage for WT *S.* Tm over the *S.* Tm Δ*aspC* mutant (**Fig. 1C**). While we observed that the overall *S*. Tm
110 burden increased over time in all three organ sites (**Fig.1D-F**), no differences in CFU recovered of each genotype
111 were observed in any location following systemic infection (**Fig. 1E-G**). Together, these data suggest that, unlike
112 *S. aureus*, *S.* Tm does not require the activity of AspC to survive in systemic sites during infection.
113

114 ***S.* Typhimurium requires AspC during murine models of gastroenteritis**

115 Before spreading to systemic sites, *S.* Tm colonizes and expands in the gastrointestinal tract[27]. We
116 previously identified that *S.* Tm gains access to the amino acid aspartate during gut inflammation due to immune
117 cell-mediated killing of the resident microbiota[16]. Secondly, we described how *S.* Tm leverages this newly
118 available aspartate to generate fumarate via the aspartate ammonia-lyase AspA, supporting anaerobic

respiration during intestinal inflammation[16]. However, how *S.* Tm deals with aspartate limitation during initial colonization before gaining access to excess aspartate during intestinal inflammation remained to be fully elucidated. Given our observations of the dispensability of AspC during systemic infection, we explored the necessity of AspC for *S.* Tm host colonization during its native route of infection, the fecal-oral route. To do so, we orally gavaged CBA/J mice with 10^9 CFU of a 1:1 mixture of WT *S*. Tm and isogenic *S.* Tm Δ*aspC*, allowing the animals to carry the infection for up to ten days (**Fig.2A**).

Following initial intestinal colonization, we observed no defects of *S.* Tm Δ*aspC* compared to WT, as we recovered equal proportions of each genotype in feces one-day p.i. (**Fig. 2B**). However, as early as five days p.i., we observed a ten-fold colonization defect for *S.* Tm Δ*aspC* compared to WT in feces, which increased to ~100-fold at nine days p.i. (**Fig.2B**). Following sacrifice, we observed that the *S.* Tm Δ*aspC* defect was restricted to the intestinal lumen, with WT *S.* Tm outcompeting the isogenic Δ*aspC* mutant in the cecum and colon content (**Fig.2C-D**). Additionally, AspC was not required for *S.* Tm survival in systemic sites such as the liver and spleen, as we recovered equal proportions of each S. Tm genotype, corroborating our IP infection observations (**Fig. 2C-D**).

To further interrogate the requirement for *asp*C during *S.* Tm gastrointestinal infection, we repeated our CBA/J mice infection model, now performing single infections. To do so, mice were orally infected with 10^9 CFU of either WT *S.* Tm or isogenic Δ*aspC* mutant, and mice carried the infection for up to ten days (**Fig. 2E**). In line with our competitive infection results, we observed no defects in the Δ*aspC* mutant at one-day p.i. as we recovered similar CFU of WT and Δ*aspC* in feces. However, starting seven days p.i., we recovered significantly less Δ*aspC S.* Tm compared to WT in the feces of infected mice by nine days p.i. (**Fig.2F**). Together, our findings suggest that *aspC* is required during *S*. Tm-induced gastroenteritis, specifically during expansion in the gut lumen.

Loss of T3SS does not significantly alter the dependence of aspC in *S*. Tm

Given our observation that the defect of Δ*aspC S.* Tm compared to the WT increased over time, in line with the onset of gastroenteritis around days seven to ten, we hypothesized this phenotype to be inflammation-dependent. To cause disease, *S.* Tm encodes two type III secretion systems, encoded by *Salmonella pathogenicity* islands 1 and 2 (T3SSs; SPI-1 & SPI-2), to invade the host epithelium and spread systemically,

147 respectively[30,31]. Additionally, loss of both SPI-1 and SPI-2 renders *S.* Tm avirulent, unable to elicit gut
148 inflammation[16]. To further interrogate the relationship between intestinal inflammation onset and the necessity of
149 *aspC* for *S.* Tm intestinal colonization, we repeated our *in vivo* competitive infection in the CBA/J model of *S.*
150 Tm-induced gastroenteritis, now using a *S.* Tm strain unable to induce intestinal inflammation through the genetic
151 inactivation of T3SSs via deletions in *invA* and *spiB*[30,31]. Briefly, we orally gavaged CBA/J mice with 10^9 CFU of
152 a 1:1 mixture of Δ*invA*Δ*spiB S.* Tm and isogenic *S.* Tm Δ*aspC*, allowing the animals to carry the infection for up
153 to ten days (**Fig. 3A**). Interestingly, compared to our wild-type background, genetic inactivation of the two T3SSs,
154 increased the fitness defect of an *aspC*-deficient *S*. Tm, demonstrating a ten-fold defect significantly higher than
155 that observed in the WT background one-day p.i. in the feces of mice (**Fig. 3B, S1**). The competitive index
156 between Δ*invA*Δ*spiB S.* Tm and isogenic Δ*invA*Δ*spiB*Δ*aspC* strains in fecal context remained steady throughout
157 infection (between 10 to 100-fold) (**Fig. 3B**). Meanwhile, the competitive index between WT *S.* Tm and isogenic
158 Δ*aspC* strain increased as the infection progressed, reaching 100-1,000-fold at day nine post-infection (**Fig. 3B**).
159 While the competitive index between *S.* Tm WT and Δ*aspC* was significantly higher than the competitive index
160 between Δ*invA*Δ*spiB* and its isogenic Δ*aspC* mutant in fecal samples at nine days post-infection (**Fig. 3B**), no
161 significant differences are observed in the competitive index between the WT and Δ*invA*Δ*spiB* backgrounds in
162 cecal (**Fig. 3C, E**) and colon (**Fig. 3D, F**) contents at 10 days p.i. In cecum and colon contents, both *S.* Tm WT
163 and Δ*invA*Δ*spiB* strain significantly outcompeted their respective Δ*aspC*-deficient mutant to similar levels (**Fig.**
164 **3C-F**).

165 Given that the *S.* Tm Δ*aspC* colonization defect increases over time (**Fig. 3B**) which correlates with the
166 onset of intestinal inflammation, we hypothesized that AspC may be more critical during anaerobic respiration,
167 which *S.* Tm relies upon for expansion in the gut lumen during intestinal disease. To explore this hypothesis, we
168 cultured WT *S.* Tm and our *aspC*-deficient mutant anaerobically *in vitro* under conditions that model the healthy
169 and inflamed gut. Specifically, we grew WT S.Tm and Δ*aspC* in LB media or NCE minimal media supplemented
170 with glucose as a carbon source in NCE minimal media supplemented with glycerol as a carbon source in the
171 presence of aspartate and inflammation-derived electron acceptors such as nitrate, as we have previously
172 performed [16]. Neither strain demonstrated an overall growth defect in the presence of LB nor NCE supplemented
173 with glucose as a carbon source, which are conditions mimicking the healthy intestine (**Fig. 4B; S2A**). However,
174 we observed an aspartate-dependent growth defect in the *S.* Tm Δ*aspC* strain upon culture in NCE

175 supplemented with nitrate, using glycerol as a carbon source, which mimics the inflamed gut (**Fig. 4C, D**).
176 Specifically, *S.* Tm Δ*aspC* demonstrated growth defects when growing under aspartate-limiting conditions (0 or
177 0.1mM aspartate). However, the *S.* Tm Δ*aspC* growth defect was ameliorated through the addition of 10mM
178 aspartate (**Fig. 4D**). We have detected similar changes in magnitude in the abundance of aspartate in the gut
179 lumen during *S*. Tm infection, increasing from 1μM up to 10μM/g of feces [16]. Similar results were obtained under
180 conditions supplemented with either tetrathionate (**Fig. 4E**) or under hypoxia (**Fig. S2B**). To corroborate our
181 observations from growth assays, we performed an *in vitro* competitive infection comparing the fitness of *S.* Tm
182 WT versus the isogenic Δ*aspC* mutant under anaerobic respiration conditions. In line with our growth assay, we
183 observed that *S.* Tm Δ*aspC* is significantly outcompeted by the WT strain in aspartate-limited conditions in which
184 the bacterium was anaerobically respiring inflammation-derived electron acceptors (**Fig. 4F, G**). The fitness
185 defect of *S.* Tm Δ*aspC* during anaerobic respiration could be abrogated by adding 10 mM aspartate. Previous
186 work in our group and others demonstrated that exposure of *S.* Tm to aspartate significantly increases the
187 expression of aspartate catabolizing enzyme AspA, dependent on the two-component system DcuRS[15,16]. To
188 account for potential differences in the expression of *aspC* in the conditions we tested, we assayed *aspC*
189 expression in *S.* Tm grown anaerobically with and without nitrate or 10 mM aspartate (**Fig. 4H**). No significant
190 differences in *aspC* expression were detected between the conditions tested (**Fig.4H**). Together, these data
191 demonstrate that a loss of *aspC* significantly hinders the ability of *S.* Tm to anaerobically respire *in vitro.*
192

193 **Loss of AspC results in altered biosynthetic processes in *S.* Tm during nitrate respiration**

194 To further explore the requirement of AspC during nitrate respiration, we compared the gene expression
195 profile of *S.* Tm WT to Δ*aspC* cultured in minimal media. Given the critical role of aspartate in the central
196 metabolism of *S.* Tm, we aimed to interrogate how aspartate deficiency influenced biosynthesis processes that
197 rely upon aspartate as a precursor. Specifically, work done in *E. coli* and *S.* Tm demonstrates that these closely
198 related bacteria can use aspartate as a precursor for the synthesis of many biological molecules, such as amino
199 acids and nucleotides (**Fig. S3A**). We were specifically interested in assessing differences in the biosynthetic
200 pathways in conditions that model the inflamed gut, as these are the conditions in which we identify an *aspC*-
201 dependent growth and fitness defect. To do so, we cultured either WT *S.* Tm or the isogenic Δ*aspC strain* in NCE
202 minimal media supplemented with 40 mM glycerol and 40 mM nitrate to evaluate differences in gene expression

203 between genotypes. First, we were able to confirm our genetic inactivation, as Δ*aspC* demonstrated a significant
204 reduction in the expression of *aspC* (**Fig. S3A-B)**. Additionally, we found that Δ*aspC* significantly upregulates
205 the aspartate importer encoded by *dcuA* but not the aspartate ammonia-lyase encoded by *aspA* (**Fig. S3C-D**).
206 Lastly, we report that loss of *aspC* in the presence of nitrate results in a significant increase in the expression of
207 genes associated with pyrimidine synthesis, such as *pyrB* and the amino acid lysine, *lysC* (**Fig. S3E-F)**. No
208 differences were observed between WT and Δ*aspC* in the expression of genes associated with methionine
209 synthesis, specifically *metL* (**Fig. S3G**). Altogether, these data suggest that genetic inactivation of *aspC* alters
210 the cellular demands of the bacterium, specifically increasing expression of genes associated with aspartate
211 uptake and synthesis of aspartate-dependent biomolecules (e.g., pyrimidines and lysine). However, our gene
212 expression analysis indicates that aspartate-dependent biosynthetic pathways remain functional in the absence
213 of AspC.
214

215 **AspC supports the central metabolism of *S*. Tm during anaerobic respiration**

216 Based on the observation that deletions in *aspC* significantly reduce *S.* Tm fitness during anaerobic
217 respiration (**Fig. 4**) as well as the limited impact of *aspC* deletion on aspartate-dependent biosynthesis pathways
218 in *S.* Tm *in vitro* under anaerobic respiration conditions (**Fig. S3E-G**), we hypothesized that AspC's role may not
219 be related to aspartate production. Instead, AspC may be required for *S.* Tm conversion of aspartate into
220 oxaloacetate (**Fig. 5A**). To explore the role of AspC in supporting *S.* Tm anaerobic respiration through
221 oxaloacetate production, we used a combination of *in vitro* supplementation using TCA intermediates and genetic
222 inactivation studies. First, we repeated our *in vitro* competitions between WT *S.* Tm and isogenic Δ*aspC* strain
223 in NCE media supplemented with 0.5% porcine mucin. We chose to perform our competitions using NCE + 0.5%
224 porcine gastric mucin to enable us to adequately model the conditions of the inflamed gut, utilizing a
225 physiologically relevant nutrient source (e.g., mucin), which allows *S.* Tm to ferment or respire available carbon
226 sources in the media. Additionally, we supplemented the NCE + 0.5% porcine mucin media with either 10 mM
227 fumarate, 10 mM succinate, or 10 mM oxaloacetate in the presence or absence of nitrate. We specifically chose
228 these TCA intermediates as they are used during both the branched chain TCA and oxidative TCA cycles (**Fig.
229 5A**). Like our previous observations in NCE minimal media supplemented with glycerol, WT *S.* Tm significantly
230 outcompeted Δ*aspC* only in mucin media supplemented with inflammation-derived electron acceptors such as

231 nitrate (**Fig. 5B-D**). If the role of AspC is to support *S.* Tm's ability to run the TCA cycle via oxaloacetate
232 production, supplementation of the media with other TCA intermediates should abrogate the *S.* Tm Δ*aspC* growth
233 defect under anaerobic respiration conditions. To test this hypothesis, we performed an *in vitro* competition in
234 NCE + 0.5% porcine mucin media supplemented with 10 mM fumarate, succinate, or oxaloacetate in the
235 presence or absence of nitrate. Notably, the addition of either of these TCA cycle intermediates to mucin media
236 did not result in a fitness defect of the Δ*aspC* mutant compared to the WT strain in the absence of nitrate (**Fig.5B-**
237 **D**). However, under anaerobic respiration conditions (e.g., mucin media + nitrate), the addition of fumarate (**Fig.**
238 **5B**), succinate (**Fig.5C**), or oxaloacetate (**Fig. 5D**) resulted in a significant reduction in the competitive advantage
239 of the WT *S.* Tm over the Δ*asp* mutant when compared to mucin media supplemented with nitrate alone (**Fig.5B-**
240 **D**). Altogether, these data suggest that loss of *aspC* results in a deficiency in TCA intermediates, namely
241 oxaloacetate, which may lead to a reduction in energy production potential during anaerobic respiration.

242 Before the onset of inflammation, *S.* Tm has been shown to rely upon the branched-chain TCA, which is
243 supported by fumarate respiration via the fumarate reductase FrdABCD[15]. However, once intestinal inflammation
244 is established and electron acceptors become available, *S.* Tm relies on the canonical oxidative TCA cycle
245 through the coordinated expression of TCA enzymes such as *sdhABCD* and *gltA* [32]. To further interrogate the
246 relationship between the progression of either the reductive branched-chain or oxidative TCA cycle and the
247 defect of the Δ*aspC S.* Tm mutant during anaerobic respiration, we constructed mutants lacking the citrate
248 synthase, *gltA*, the first component of the succinate dehydrogenase, *sdhA*, and the fumarate reductase,
249 *frdABCD*. These genes represent significant steps of the branched chain reductive (FrdABCD) and oxidative
250 (GltA & SdhA) TCA cycles in *S.* Tm (**Fig. 5A**). To understand the role of AspC in the TCA enzyme-deficient strain
251 backgrounds, we constructed *S.* Tm isogenic mutants lacking *aspC,* Δ*gltA*Δ*aspC,* Δ*sdhA*Δ*aspC,* and
252 Δ*frdABCD*Δ*aspC,* respectively. We hypothesized, based on our supplementation studies, that interruption of the
253 TCA cycle progression via deletions in *gltA* and *sdhA* but not *frdABCD* would abrogate the defect of *S.* Tm Δ*aspC*
254 during nitrate respiration. To test this hypothesis, we performed an *in vitro* competition in 0.5% porcine mucin
255 media in the presence or absence of nitrate, specifically competing *S.* Tm WT, Δ*frdABCD,* Δ*sdhA,* Δ*gltA* with their
256 respective isogenic *aspC* mutants.

257 First, to assess the requirement for *aspC* during the reductive branched-chain TCA cycle in *S.* Tm, we
258 compared the competition index of our mutant Δ*frdABCD*: Δ*frdABCD*Δ*aspC* to WT:Δ*aspC* in minimal mucin media

259 without nitrate. Interestingly, we observed a significantly increased fitness defect of Δ*frdABCD* Δ*aspC* compared
260 to the Δ*frdABCD* isogenic control (CI~10) (**Fig. S4A**) over that of WT vs. Δ*aspC* (CI~1). In line with the literature
261 that *frdABCD* is significantly downregulated during exposure to nitrate, we observed no significant difference in
262 the fitness defect of an Δ*aspC* mutant during nitrate respiration in the *S.* Tm background lacking *frdABCD* (**Fig.**
263 **5E**). Together, these data suggest that AspC supports the branched chain TCA cycle during which fumarate
264 respiration occurs and that FrdABCD is not required for the AspC-mediated effect on the *S.* Tm oxidative TCA
265 cycle during nitrate respiration.

266 To determine the requirement for *sdhA* and *gltA* to the AspC-mediated support of *S.* Tm growth during
267 the branched chain TCA cycle, we compared the competition index of our mutants Δ*sdhA*: Δ*sdhA*Δ*aspC* or Δ*gltA*:
268 Δ*gltA*Δ*aspC* to WT: Δ*aspC* in 0.5% porcine mucin media without nitrate. Loss of *aspC* conferred no fitness defect
269 in S. Tm strains lacking *sdhA* and *gltA* (**Fig. S4B**). Conversely, loss of *sdhA* or *gltA* significantly abrogated the
270 fitness defect of a *S.* Tm Δ*aspC* mutant when compared to the isogenic WT background when strains were grown
271 in 5% porcine mucin media supplemented with nitrate, a condition that enables S. Tm to run the oxidative TCA
272 cycle (**Fig. 5F-G**). Together, our results using a genetic approach relying on the deletion of genes in *S.* Tm
273 involved in the TCA cycle complement the results from the TCA cycle intermediate supplementation experiments
274 (**Fig. 5B-D**) and pinpoint the requirement for *aspC* to support the progression of the oxidative but not reductive
275 branched-chain TCA cycle in *S.* Tm.
276

277 **DISCUSSION**

278 Herein, this study establishes a role for the aspartate aminotransferase, AspC, in the expansion of
279 *Salmonella* Typhimurium in the mammalian gut. Using intraperitoneal and intragastric infection routes, we report
280 that AspC is only required during expansion in the intestinal lumen and is dispensable in systemic sites such as
281 the liver and spleen. Additionally, we find that the necessity of AspC for *S.* Tm intestinal survival to be potentially
282 independent of the main virulence program of *S.* Tm, the two T3SSs. However, we observe the loss of the ability
283 to invade, and intracellular replication significantly increases the defect of an isogenic *aspC*-deficient strain one
284 d.p.i. Thus, our data suggest *S.* Tm may subvert initial aspartate starvation in the healthy gut by invading the gut
285 epithelium. This hypothesis is in line with work by Popp *et al.* that demonstrates that AspC is not required for
286 invasion or intracellular replication within HeLa cells[18]. Granted, there may be cell-type-specific differences in

287 nutrient availability between uterine epithelial and intestinal epithelial cells, and future work should aim to
288 understand the nutrient requirements between different infection-relevant organ sites.

289 Our study indicates that a loss of *aspC* results in altered metabolic demands for the pathogen, as
290 determined by qPCR, *in vitro* supplementation, and genetic inactivation of key TCA enzymes. We observe that
291 loss of AspC results in increased expression of genes encoding enzymes associated with the import and
292 utilization of aspartate for the synthesis of amino acids and nucleotides. However, these alterations have a limited
293 induction, resulting in less than a 2-fold change, suggesting tight control of these central metabolic processes.
294 Alternatively, we find that *S.* Tm Δ*aspC* demonstrates a significant growth defect under *in vitro* conditions that
295 promote the reductive branched chain and oxidative TCA cycle. Thus, suggesting one possible explanation for
296 the defect of *S.* Tm Δ*aspC* in gut expansion is the inability of this strain to take advantage of the disruption in the
297 metabolic landscape of the gut during gastroenteritis.

298 Lastly, while we do not observe major differences in the competitive fitness of *S.* Tm Δ*aspC* in a
299 background lacking *frdABCD* under *in vitro* conditions supporting anaerobic respiration, we cannot rule out the
300 possibility of the fumarate reductase FrdABCD aiding in driving the oxidative TCA forward, as its expression is
301 induced in *S.* Tm under *in vitro* anaerobic growth conditions characterized by the presence of excess aspartate
302 and nitrate which resemble the growth conditions encountered by the pathogen in the inflamed gut[16]. Future
303 work should aim to untangle the relationship between FrdABCD and SdhABCD in supporting the pathogenesis
304 and expansion of *S.* Tm in the mammalian gut.

305 Altogether, our findings expand our understanding of *S.* Tm aspartate metabolism and its influence on
306 survival in different organ sites. Studies on bacterial metabolism are poised to elucidate previously unknown
307 aspects of pathogenic bacterial survival and inform therapeutic strategies targeting these essential metabolic
308 pathways.

309

310 **MATERIALS & METHODS**

311 ***In vitro***

312 **Bacterial culture**

313 *S.* Typhimurium IR715 strains were routinely grown aerobically at 37°C in LB broth (10 g/L tryptone, 5
314 g/L yeast extract, 10 g/L sodium chloride) or on LB agar plates (10 g/L tryptone, 5 g/L yeast extract, 10 g/L sodium

315 chloride, 15 g/L agar). When appropriate, agar plates and media were supplemented with 30 μg/mL
316 chloramphenicol (Cm), 100 μg/mL carbenicillin (Carb), 100 μg/mL kanamycin (Km), or 50 μg/mL nalidixic acid
317 (Nal). For growth under anaerobic conditions, No-carbon-E (NCE) minimal medium (28 mM KH_2PO_4, 28 mM
318 $K_2HPO_4 \cdot 3H_2O$ and 16 mM $NaNH_4HPO_4 \cdot 4H_2O$) supplemented with 1 mM $MgSO_4$, 0.1% Casamino acids and 1%
319 Vitamin and Trace mineral solutions (American Type Culture Collection) was used. As a sole carbon source,
320 glucose (5mM) or glycerol (40 mM) was added to the bacterial culture in addition to L-aspartate (0.1-
321 10 mM). When stated otherwise, bacteria were cultured in Mucin minimal media, NCE minimal media (28 mM
322 KH_2PO_4, 28 mM $K_2HPO_4 \cdot 3H_2O$ and 16 mM $NaNH_4HPO_4 \cdot 4H_2O$) supplemented with 0.5% Porcine Gastric Mucin
323 (Type II) (ThermoFischer) supplemented with 40mM sodium nitrate, 10mM sodium fumarate, succinic acid, or
324 oxaloacetic acid.
325
326 **Mutant generation**
327 Mutant construction was done via lambda red recombination as previously described[34]. In brief, primers
328 were designed to include 40bps homologous regions upstream and downstream of the gene of interest and used
329 to amplify the Kan^R cassette in pKD13. Kan cassette was amplified, and PCR product DpnI was treated and
330 purified before electroporation into *S*. Tm IR715 harboring the helper plasmid pKD46 grown in the presence of
331 0.1M L-arabinose. The transformation was plated on LB agar supplemented with Kanamycin and incubated
332 overnight at 37°C, and colonies were checked via PCR. Following insertion confirmation, insertion was pushed
333 into a clean background as described[35] before transforming with pCP20 to remove the Kan^R cassette. Mutants
334 were PCR verified.
335
336 **Growth Kinetics**
337 Bacteria were streaked out onto fresh selective agar plates and incubated overnight. Single colonies
338 were taken and cultured in LB broth supplemented with appropriate antibiotics in biological triplicate for three
339 independent experiments. Overnight cultures were then back diluted 1:100 for 1-2 hours in 5mL of fresh LB broth
340 supplemented with antibiotics until the bacteria reached the mid-log phase. Cultures were then washed and
341 normalized to an OD_{600}=1. Cultures were then inoculated into a final volume of 200uL per well of pre-reduced
342 media to a final OD_{600}=0.01, shaking continuously, incubated at 37, and OD_{600} measured every hour.

343

344 **Gene expression analysis**

345 Bacteria were streaked out fresh onto selective agar plates and incubated overnight. Single colonies
346 were taken, and cultures for biological replicates of n=5 in three independent experiments were grown overnight.
347 Overnight cultures were diluted 1:100 for 2-3 hours to reach the mid-log phase of growth, harvested, and washed.
348 Cultures normalized and inoculated into NCE minimal media containing ± 10mM aspartate and ± 40mM nitrate,
349 pH normalized to 7.2. Bacteria were then incubated for 4 hours anaerobically at 37°C before being harvested
350 and RNA extracted using Max Bacterial-RNA Extraction Reagent and TRIzol combined with the Invitrogen
351 PureLink RNA mini-kit following the manufacturer's instructions.

352

353 ***In vitro* competitive infections**

354 Bacterial strains were struck out onto selective agar plates and incubated overnight. Single colonies takenand
355 cultures for biological replicates of n=5 in three independent experiments were grown overnight. Overnight
356 cultures were then diluted 1:100 for 2-3 hours to reach the mid-log phase of growth, harvested, and washed.
357 Cultures were then normalized and inoculated into pre-reduced NCE or NCE+0.5% Porcine Gastric Mucin (type
358 II) at a final bacterial concentration of $1x10^4$CFU/mL. Samples collected before and after 18hrs anaerobic
359 incubation at 37°C. Samples serially diluted and plated on LB + Kan and LB + Cm, CFU enumerated, and CI
360 calculated for both time points and normalized to calculate competition index of inoculum.

361

362 **Mouse models of *S.* Tm infection**

363 All animal experiments in this study were approved by the Institutional Animal Care and Use Committee
364 at Vanderbilt University Medical Center. Female CBA were obtained from the Jackson Laboratory. The age at
365 the beginning of the experiment was 6-7 weeks for all CBA. Conventional mice were housed in individually
366 ventilated cages with ad libitum access to water and chow (Envigo Global 16% Protein Rodent Diet). Unless
367 stated otherwise, a minimum of 6 mice were used based on variability observed in previous experiments. All
368 mice were monitored twice per day, and cage bedding was changed every two weeks. At the end of the
369 experiments, mice were humanely euthanized using carbon dioxide inhalation and cervical dislocation. Animals

370 that had to be euthanized for humane reasons before reaching the predetermined time point were excluded from
371 the analysis.
372
373 *Intraperitoneal infection*
374 7-week-old CBA/J mice were purchased from Jackson Labs Inc., infected with 10^4 C.F.U. of each strain,
375 and carried for 96 hours post-infection before sacrifice. Mice were weighed every day post-infection. At sacrifice,
376 peritoneal lavage, liver, spleen, and intestinal content were collected and plated for bacterial burden via serial
377 dilution onto LB agar supplemented with either Chloramphenicol or Kanamycin, dependent on strain background.
378
379
380 *Intragastric infection*
381 7-week-old CBA/J mice were purchased from Jackson Labs Inc. and were infected intragastrically with
382 10^9 C.F.U. of each strain for a single-strain infection or a 1:1 ratio of WT and respective isogenic mutant strains
383 for competitive infections. Post-infection mice were maintained for ten days weighing daily and collecting feces
384 every other day for bacterial burden enumeration. At sacrifice, mice were euthanized, and liver, spleen, and
385 intestinal tissue and content were taken for bacterial enumeration via homogenization and serial dilution. Tissue
386 was taken for histopathology evaluation.
387
388 **Quantification and Statistical analysis**
389 Statistical data analysis was performed using GraphPad PRISM. Fold changes of ratios (bacterial
390 competitive index and mRNA levels), and bacterial numbers were transformed logarithmically prior to statistical
391 analysis. An unpaired or paired Student's t test was used on the transformed data to determine whether
392 differences between groups were statistically significant ($p < 0.05$). When more than two treatments were used,
393 statistically significant differences between groups were determined by one-way ANOVA followed by Tukey's
394 HSD test (between > 2 groups).
395
396 **Acknowledgments**

N.G.S. was supported by NIH T32 Training Grant (T32ES007028-46) and HHMI Gilliam Fellowship (GT15104). J.O. was supported by NIH T32 Training Grant (T32AI095202-15). K.M.J. was supported by NIH T32 Training Grant (T32GM137793-05). M.X.B is a HHMI Freeman Hrabowski Scholar. Work in M.X.B.'s laboratory was supported by VDDRC Pilot and Feasibility grant P30 058404, the NIH (R01DK131104-01 and 1R01AI168302-01A1), The Pew Charitable Trusts (2022-A-19568), and the Burroughs Wellcome Fund (022792).

Author contributions

Conceptualization, N.G.S., and M.X.B.; Methodology, N.G.S, and M.X.B.; Investigation, N.G.S., M.X.B., H.F.A., J.O., K.M.J.; Writing – Original Draft, N.G.S.; Writing – Review & Editing, N.G.S., M.X.B.; Funding Acquisition, M.X.B.; Resources, M.X.B.; Supervision, M.X.B.

FIGURE LEGENDS

Figure 1: ***S*. Tm does not require AspC for systemic survival following intraperitoneal injection**.

CBA/J mice were infected with a competitive 1:1 ratio of WT and *aspC*-deficient *S*. Tm IR715, via intraperitoneal injection at a dose of 10^4 CFU. Mice were allowed to carry the pathogen for pre-determined time points, prior to human euthanasia and sample collection. (A) Infection Schematic. (B) Weight-loss percentage compared to inoculation weight, of mice sacrificed three-, four-, and five-days post-infection. (C) Competitive index of inoculum at each time point based on the proportion of *S*. Tm in liver and spleen homogenate as well as intraperitoneal lavage fluid. (D) *S.* Tm burden of each genotype in the Liver. (E) *S.* Tm burden of each genotype in the CFU/g in spleen. (F) *S.* Tm burden of each genotype in the intraperitoneal fluid following lavage. N=6 per time point. Geometric mean with geometric SD. Multiple t-test.

Figure 2: Deletion of *aspC* results in a significant expansion defect only in the cecum and colon, during murine model of gastroenteritis. To interrogate the necessity the AspC through the canonical fecal-oral route of infection, we then gavaged CBA/J mice with a competitive 1:1 ratio of our WT and Δ*aspC* mutant. (A) Schematic for competitive *in vivo* infection. (B) Competition index of inoculum over time in feces. (C) Competition index of inoculum ten d.p.i. from systemic and gut lumen samples of infected mice. To corroborate our observations, we repeated our infection, with either of our strains in isolation. (D) Schematic for single infection. (E) *S*. Tm burden in feces overtime in mice infected with either WT or Δ*aspC* mutant. (F) Pathohistological scoring

427 of liver, spleen, and cecal tip of WT or *aspC*-deficient infected CBA/J mice ten d.p.i. N=6 per condition. Geometric
428 mean and Geometric SD. Paired-end (D) or Unpaired T-test (E).
429
430 **Figure 3: Genetic inactivation T3SSs results in a colonization defect of Δ*aspC* but does not alter overall**
431 **expansion defect.** Based on our findings during single and competitive infections, we then wanted to understand
432 if the necessity of AspC was related to the ability of *S*. Tm to invade and systemically spread within the murine
433 host. To do so, we constructed isogenic mutants in an avirulent background and repeated our competitive
434 infection compared to that of a WT background, again in CBA mice. (A) Infection schematic of competitive
435 infection. (B) Competitive index of inoculum in feces over the course of the infection. Day 3 samples were not
436 collected. (C) Competitive index of inoculum in feces one d.p.i. (D) Competitive index of inoculum in cecal
437 content, and (E) colon content (F) *S*. Tm burden of each genotype in cecal content and colon content ten d.p.i.
438 N=6 per background, Paired- or Unpaired T-test. P=*, <0.05; **,<0.01; ***, <0.001; ****, <0.0001.
439
440 **Figure 4**: **AspC is required for *S*. Tm growth under aspartate limiting conditions, confers a significant**
441 **fitness cost during anaerobic respiration, and is constitutively expressed by replicating cells**. Given our
442 findings that the competitive defect we observed increased over the course of infection, and that S. Tm requires
443 the ability to respire during this time point, we aimed to interrogate the relationship of the function of AspC during
444 fermentation and anaerobic respiration. (A) Schematic of the enzymatic role of AspC in *S.* Tm. (B) Anaerobic
445 growth of WT and *aspC* deficient *S*. Tm in NCE minimal media supplemented with 5mM Glucose. (C) Anaerobic
446 growth of WT and *aspC* deficient *S*. Tm in NCE minimal media supplemented with 40mM Glycerol with or without
447 40mM Nitrate. (D) Anaerobic growth of WT and *aspC* deficient *S*. Tm in NCE minimal media supplemented with
448 (+) 0.1mM or (+++) 10mM Aspartate with Glycerol and Nitrate. (E) *In vitro* competition of WT vs *aspC* in NCE
449 supplemented with 40mM Tetrathionate, 10mM Aspartate, and 40mM Glycerol. (F) *In vitro* competition of WT vs
450 *aspC* in NCE supplemented with 40mM Nitrate, 10mM Aspartate, and 40mM Glycerol. (G) Relative expression
451 of *aspC* in WT *S*. Tm cultured anaerobically for 4hrs in media supplemented with 10mM Aspartate, 40mM
452 Glycerol, and 40mM Nitrate. N=3-10 per condition, at least 2 independent experiment for each, Geometric mean
453 with geometric SD. Multiple t-test or One-way ANOVA, P=*, <0.05; ****, <0.0001.
454

455

456 **Figure 5: AspC is required for anaplerosis of the TCA by *S*. Tm during anaerobic respiration, *in vitro*.**

457 Based on the findings that loss of *aspC* significantly reduces *S*. Tm growth and fitness during anaerobic
458 respiration of inflammation-derived electron acceptors, we aimed to understand if aspartate conversion into
459 oxaloacetate via AspC fueled pathogen growth. (A) Tricarboxylic acid cycle. (B-D) To confirm the role of AspC
460 during nitrate respiration, we performed competitive infections in the presence of absence of TCA intermediates.
461 Competitive index of inoculum between WT and Δ*aspC S.* Tm in the presence or absence of nitrate
462 supplemented with (B) Fumarate (C) Succinate, and (D) Oxaloacetate. (E-F) Additionally, we repeated our
463 competitive infections now in backgrounds lacking the enzymes responsible for the utilization of: (E) Fumarate
464 via fumarate reductase; (F) succinate via succinate dehydrogenase subunit A; (G) oxaloacetate via citrate
465 synthase. N= 10 per condition. One-way ANOVA or T-test. P=*, <0.05; **,<0.01; ***, <0.001; ****, <0.0001

466

467 **References**

468 1. Jacobson, A. *et al.* A gut commensal-produced metabolite mediates colonization resistance to
469 Salmonella infection. *Cell Host Microbe* **24**, 296–307 (2018).
470 2. Van Der Waaij, D., Berghuis-De, J. M. & Lekkerkerk-Van Der Wees, J. E. C. *Colonization*
471 *Resistance of the Digestive Tract in Conventional and Antibiotic-Treated Mice*. *J. Hyg., Camb*
472 vol. 69 (1971).
473 3. Caballero-Flores, G., Pickard, J. M., Fukuda, S., Inohara, N. & Núñez, G. An Enteric Pathogen
474 Subverts Colonization Resistance by Evading Competition for Amino Acids in the Gut. *Cell Host*
475 *Microbe* **28**, 526-533.e5 (2020).
476 4. Osbelt, L. *et al.* Klebsiella oxytoca causes colonization resistance against multidrug-resistant
477 K. pneumoniae in the gut via cooperative carbohydrate competition. *Cell Host Microbe* 1–17
478 (2021) doi:10.1016/j.chom.2021.09.003.
479 5. Eberl, C. *et al.* E. coli enhance colonization resistance against Salmonella Typhimurium by
480 competing for galactitol, a context-dependent limiting carbon source. *Cell Host Microbe* 1–13
481 (2021) doi:10.1016/j.chom.2021.09.004.
482 6. Sommer, F. & Bäckhed, F. The gut microbiota-masters of host development and physiology. *Nat*
483 *Rev Microbiol* **11**, 227–238 (2013).
484 7. Takiishi, T., Fenero, C. I. M. & Câmara, N. O. S. Intestinal barrier and gut microbiota: Shaping
485 our immune responses throughout life. *Tissue Barriers* **5**, (2017).
486 8. Litvak, Y., Byndloss, M. X. & Bäumler, A. J. Colonocyte metabolism shapes the gut microbiota.
487 *Science (1979)* **362**, 6418 (2018).
488 9. Bamba, S. *et al.* Altered gut microbiota in patients with small intestinal bacterial overgrowth.
489 *Journal of Gastroenterology and Hepatology (Australia)* **38**, 61–69 (2023).
490 10. Cheng, H. Y., Ning, M. X., Chen, D. K. & Ma, W. T. Interactions between the gut microbiota and
491 the host innate immune response against pathogens. *Front Immunol* **10**, 1–11 (2019).
492 11. Shelton, C. D. *et al.* An early-life microbiota metabolite protects against obesity by regulating
493 intestinal lipid metabolism. *Cell Host Microbe* **31**, 1604-1619.e10 (2023).
494 12. Yoo, W. *et al.* High-fat diet-induced colonocyte dysfunction escalates microbiota-derived
495 trimethylamine N-oxide. *Science (1979)* **373**, 813–818 (2021).

13. Diaz-ochoa, V. E. *et al.* Salmonella mitigates oxidative stress and thrives in the inflamed gut by evading calprotectin-mediated manganese sequestration. *Cell Host Microbe* **19**, 814–825 (2016).
14. Schofield, W. B., Zimmermann-Kogadeeva, M., Zimmermann, M., Barry, N. A. & Goodman, A. L. The Stringent Response Determines the Ability of a Commensal Bacterium to Survive Starvation and to Persist in the Gut. *Cell Host Microbe* **24**, 120-132.e6 (2018).
15. Nguyen, B., Hartl, J., Sunagawa, S., Christen, B. & Hardt, W. Import of Aspartate and Malate by DcuABC Drives H 2 / Fumarate Respiration to Promote Initial Salmonella Gut-Lumen Colonization in Mice. *Cell Host Microbe* **27**, 1–15 (2020).
16. Yoo, W. *et al.* Salmonella Typhimurium expansion in the inflamed murine gut is dependent on aspartate derived from ROS-mediated microbiota lysis. *Cell Host Microbe* **32**, 887-899.e6 (2024).
17. Liu, F. *et al.* AspC-mediated aspartate metabolism coordinates the Escherichia coli cell cycle. *PLoS One* **9**, (2014).
18. Popp, J. *et al.* Role of host cell-derived amino acids in nutrition of intracellular Salmonella enterica. *Infect Immun* **83**, 4466–4475 (2015).
19. Vayena, E. *et al.* Metabolic network reconstruction as a resource for analyzing Salmonella Typhimurium SL1344 growth in the mouse intestine. *PLoS Comput Biol* **21**, (2025).
20. Hinojosa-Leon', M., Dubourdieul, M., Sanchez-Crispin', J. A. & Chippaux, M. Tetrathionate reductase of Salmonella typhimurium: a molybdenum containing enzyme. *Biochem Biophys Res Commun* **136**, 577–581 (1986).
21. Lopez, C. A., Rivera-Chávez, F., Byndloss, M. X. & Bäumler, A. J. The periplasmic nitrate reductase NapABC supports luminal growth of Salmonella enterica serovar typhimurium during colitis. *Infect Immun* **83**, 3470–3478 (2015).
22. Rivera-Chávez, F. *et al.* Energy taxis toward host-derived nitrate supports a salmonella pathogenicity island 1-independent mechanism of invasion. *mBio* **7**, (2016).
23. Potter, A. D. *et al.* Host nutrient milieu drives an essential role for aspartate biosynthesis during invasive Staphylococcus aureus infection. doi:10.1073/pnas.1922211117/-/DCSupplemental.
24. WHO. *WHO Estimates of the Global Burden of Foodborne Diseases: Foodborne Disease Burden Epidemiology Reference Group 2007-2015*. (World Health Organization, 2015).
25. Palmer, A. D. & Slauch, J. M. Mechanisms of Salmonella pathogenesis in animal models. *Human and Ecological Risk Assessment* vol. 23 1877–1892 Preprint at https://doi.org/10.1080/10807039.2017.1353903 (2017).
26. Santos, R. L. *et al. Animal Models of Salmonella Infections: Enteritis versus Typhoid Fever*. (2001).
27. Sanderson, K. E., Liu, S. L., Tang, L. & Johnston, R. N. Salmonella Typhi and Salmonella Paratyphi A. in *Molecular Medical Microbiology* 1275–1306 (Elsevier, 2014). doi:10.1016/B978-0-12-397169-2.00071-8.
28. Broz, P., Ohlson, M. B. & Monack, D. M. Innate immune response to Salmonella typhimurium, a model enteric pathogen. *Gut Microbes* **3**, 62–70 (2012).
29. Van Dyk, T. K. & Larossa, R. A. *Sensitivity of a Salmonella Typhimurium AspC Mutant to Sulfometuron Methyl, a Potent Inhibitor of Acetolactate Synthase II*. *JOURNAL OF BACTERIOLOGY* vol. 165 (1986).
30. Hapfelmeier, S. *et al. The Salmonella Pathogenicity Island (SPI)-2 and SPI-1 Type III Secretion Systems Allow Salmonella Serovar Typhimurium to Trigger Colitis via MyD88-Dependent and MyD88-Independent Mechanisms 11-Dependent and MyD88-Independent Signaling to Epithelial Cells and SPI-2-Dependent Intracellular Proliferation in the Lamina Propria Triggering MyD88-Dependent Innate Immune Responses*. *The Journal of Immunology* vol. 174 http://journals.aai.org/jimmunol/article-pdf/174/3/1675/1196409/1675.pdf (2005).
31. Coombes, B. K. *et al.* Analysis of the contribution of Salmonella pathogenicity islands 1 and 2 to enteric disease progression using a novel bovine ileal loop model and a murine model of infectious enterocolitis. *Infect Immun* **73**, 7161–7169 (2005).

548 32. Spiga, L. *et al.* An oxidative central metabolism enables Salmonella to utilize microbiota-derived
549 succinate. *Cell Host Microbe* **22**, 291–301 (2018).
550 33. Mercado-lubo, R., Gauger, E. J., Leatham, M. P., Conway, T. & Cohen, P. S. A Salmonella
551 enterica Serovar Typhimurium Succinate Dehydrogenase / Fumarate Reductase Double Mutant
552 Is Avirulent and Immunogenic in BALB / c Mice. **76**, 1128–1134 (2008).
553 34. Datsenko, K. A. & Wanner, B. L. One-step inactivation of chromosomal genes in Escherichia
554 coli K-12 using PCR products. *Proc Natl Acad Sci U S A* **97**, 6640–6645 (2000).
555 35. Bochner, B. R. *Curing Bacterial Cells of Lysogenic Viruses by Using Ucb Indicator Plates*. vol.
556 Sept/Oct (1984).
557
558
559

560 **FIGURE 1**
561

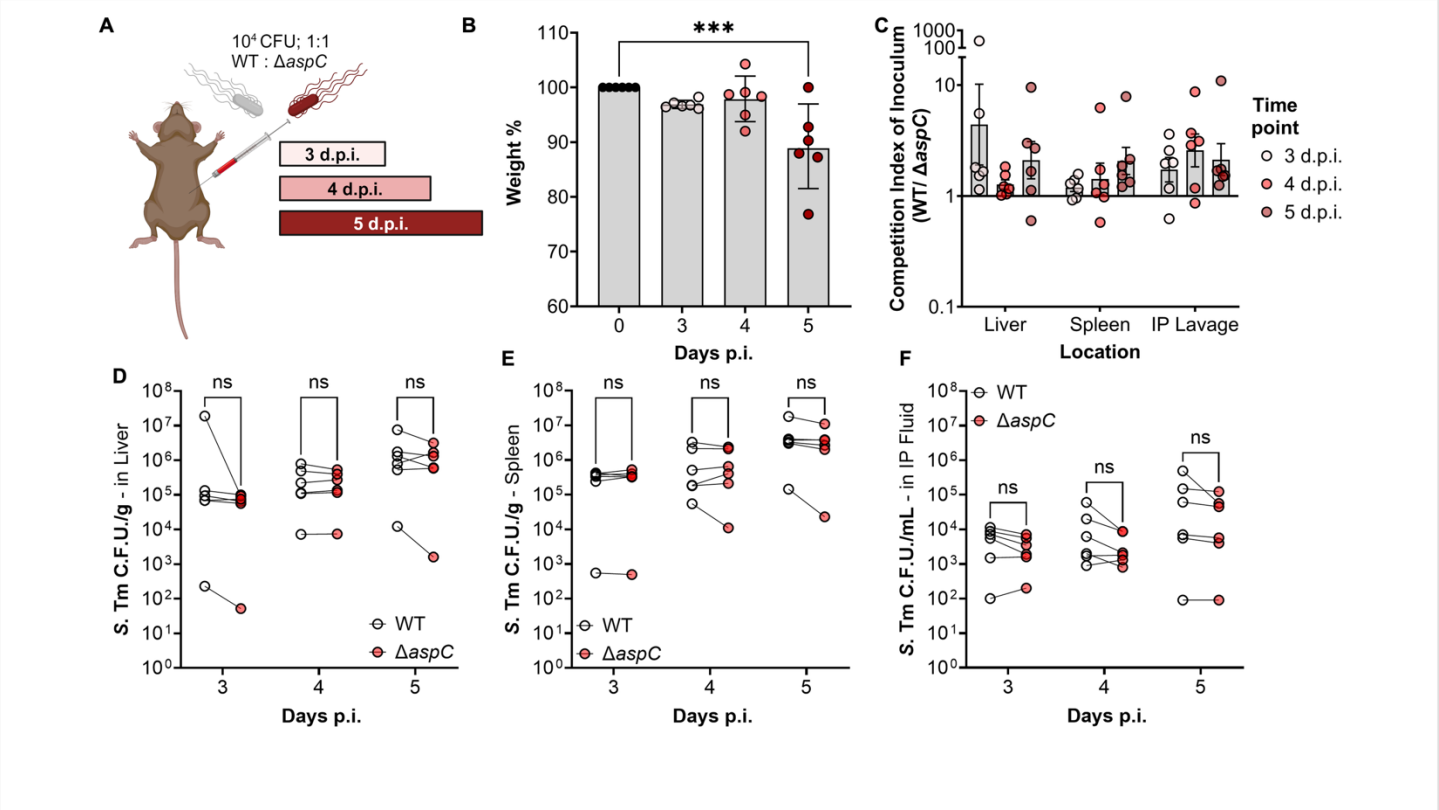

562
563
564

565 **FIGURE 2**
566

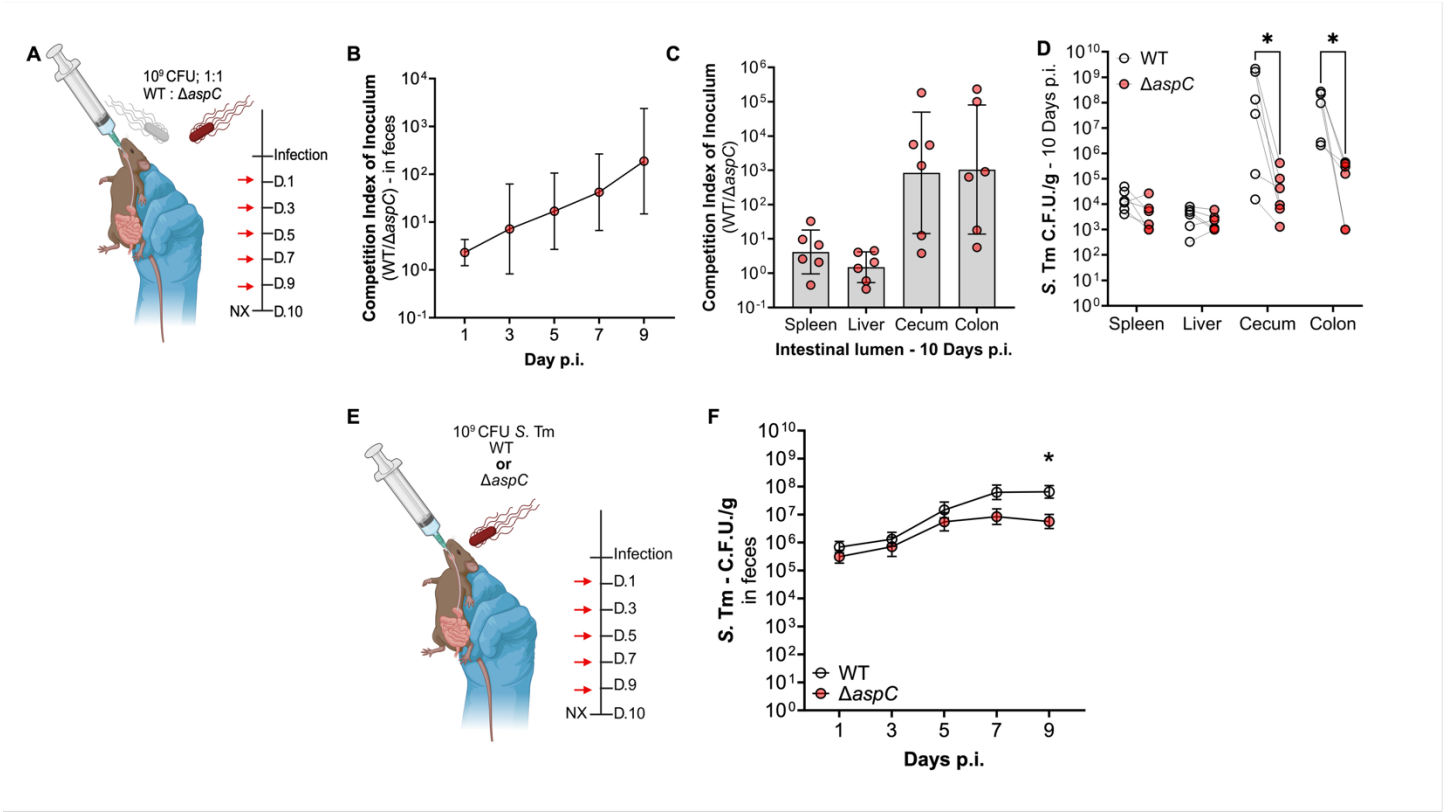

567
568
569

570 **FIGURE 3**
571

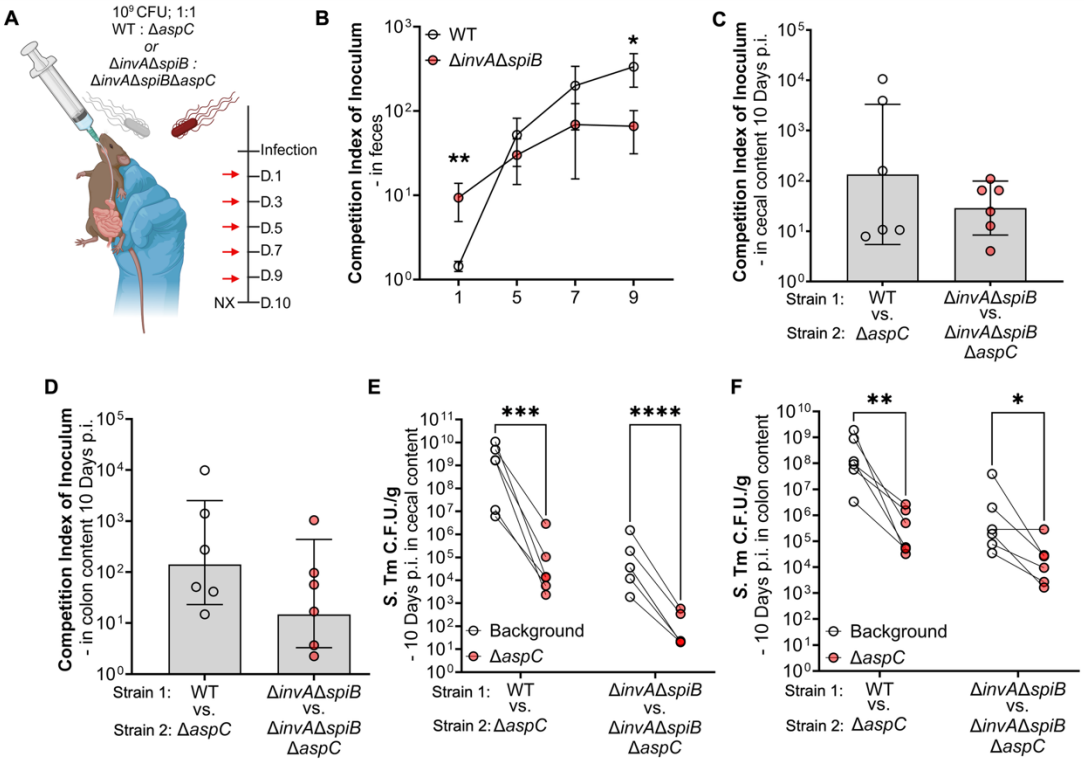

572
573
574

575 **FIGURE 4**
576

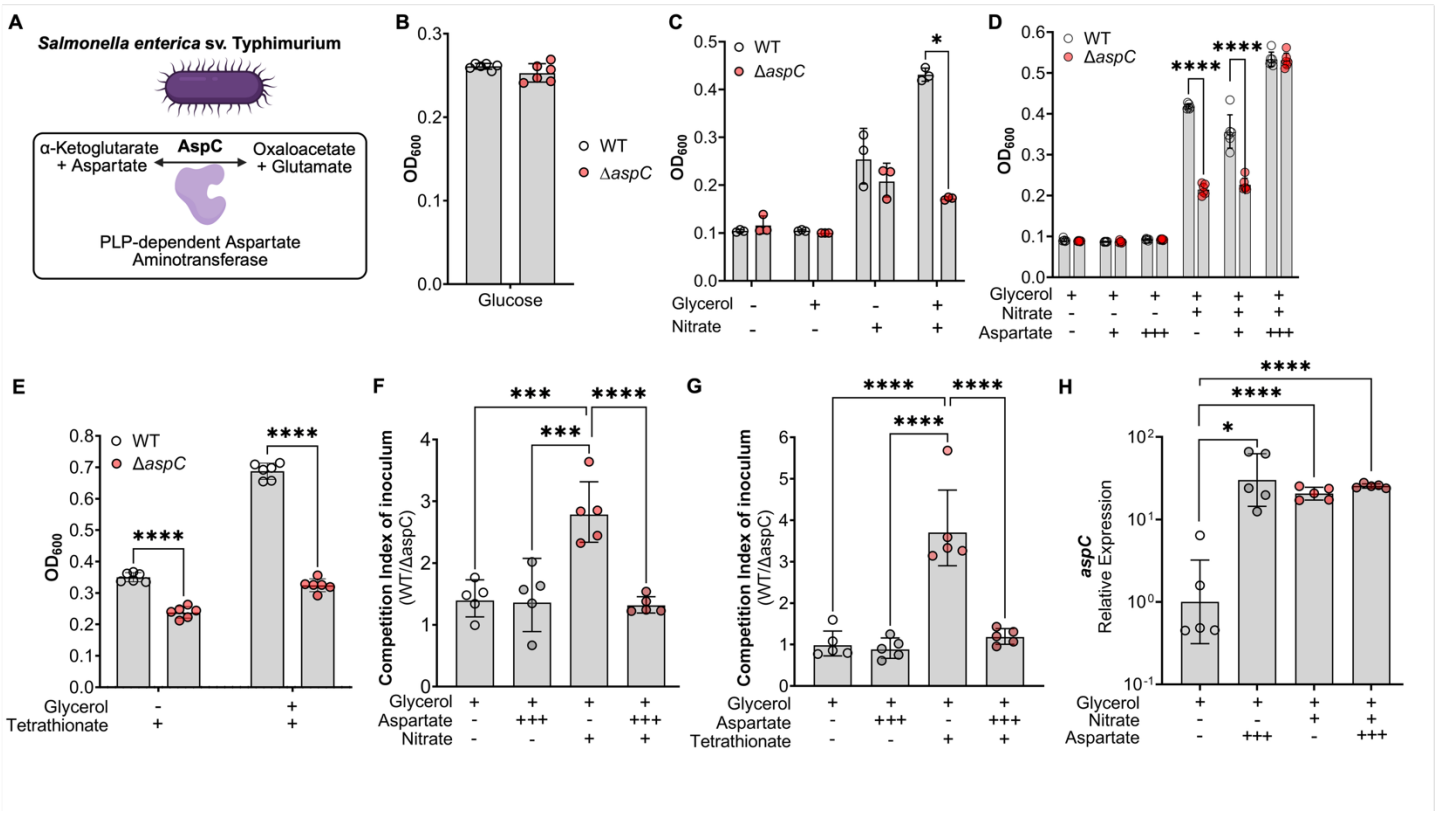

577
578
579

580 **FIGURE 5**

581

582

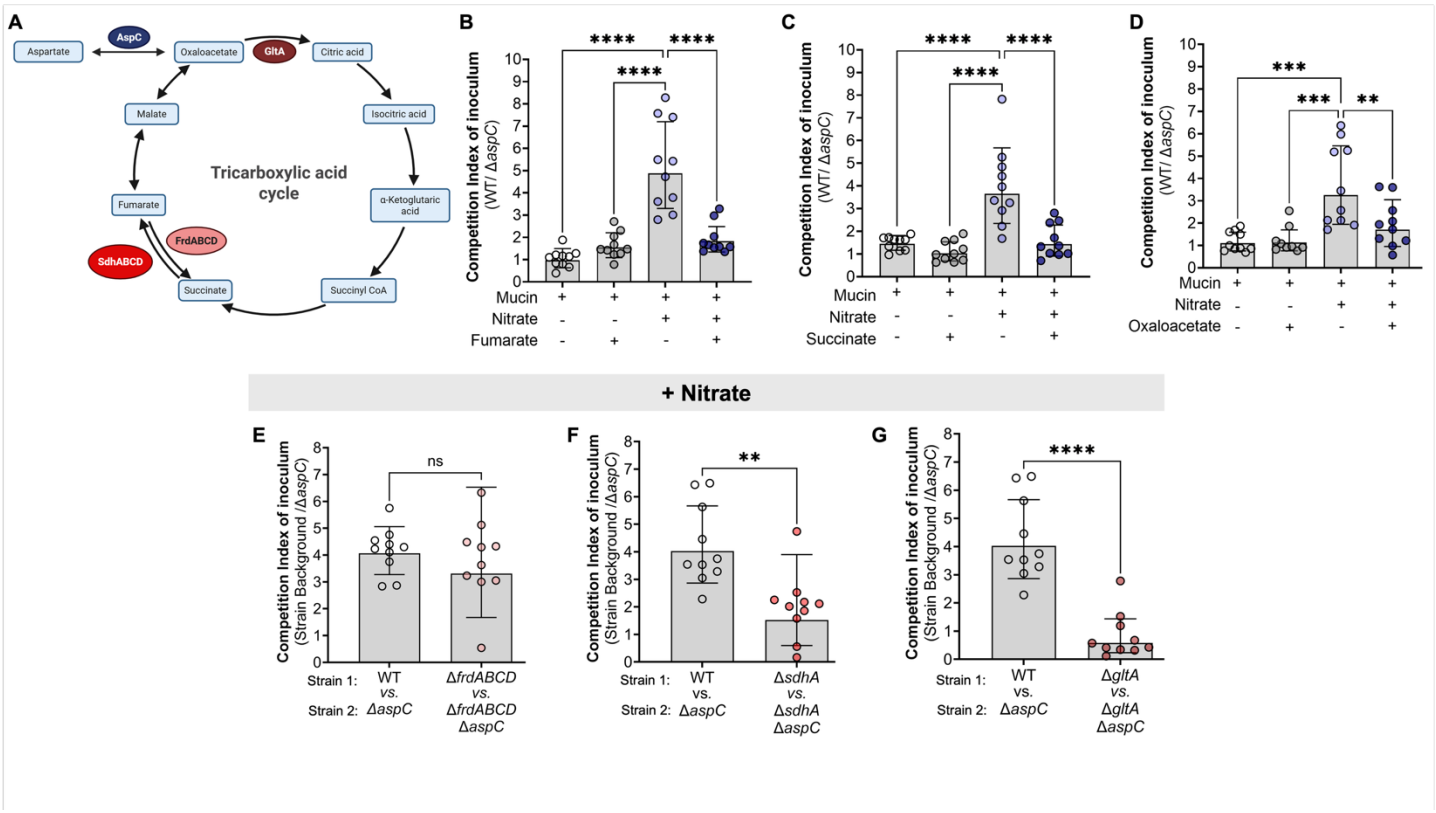

583

584

585

586 **SUPPLEMENTARY MATERIALS**

587 **Supplementary Table 1: Bacterial strains and plasmids used in this study.**

Bacterial Strain	**Source**	**Identification**
S. Typhimurium, IR715 ATCC 14028S Nal^R	Stojiljkovic et al.[47]	IR715
S. Typhimurium, IR715 Δ*phoN*::Tn*10d*-Cm^R	Faber et al.[48]	FF176
S. Typhimurium, IR715 Δ*phoN*::Km^R	Kingsley et al.[49]	AJB715
S. Typhimurium, IR715 Δ*aspC*::Km^R	This study	NS42
S. Typhimurium, IR715 Δ*aspC*	This study	NS43
S. Typhimurium, IR715 Δ*frdABCD*	This study	WJ28
S. Typhimurium, IR715 Δ*frdABCD*Δ*phoN*::Tn*10d*-Cm^R	This study	WJ30
S. Typhimurium, IR715 Δ*invA*Δ*spiB*	Rivera-Chávez et al.[50]	SPN487
S. Typhimurium, IR715 Δ*invA*Δ*spiB*Δ*aspC*::Km^R	This study	NS301
S. Typhimurium, IR715 Δ*invA* Δ*spiB* Δ*phoN*::Tn*10d*-Cm^R	This study	WJ52
S. Typhimurium, IR715 Δ*invA*Δ*spiB*Δ*aspC*	This study	NS311
S. Typhimurium, IR715 Δ*invA* Δ*spiB*Δ*aspC*Δ*phoN::*Km^R	This study	NS313
S. Typhimurium, IR715 Δ*sdhA*::Km^R	This study	NS314
S. Typhimurium, IR715 Δ*gltA*::Km^R	This study	NS315
S. Typhimurium, IR715 Δ*sdhA*Δ*aspC*::Km^R	This study	NS316
S. Typhimurium, IR715 Δ*gltA*Δ*aspC*::Km^R	This study	NS317
S. Typhimurium, IR715 Δ*sdhA*ΔphoN::Tn10d-Cm^R	This study	NS318
S. Typhimurium, IR715 Δ*gltA*Δ*phoN*::Tn10d-Cm^R	This study	NS319
S. Typhimurium, IR715 Δ*sdhA*Δ*aspC*Δ*phoN*::Km^R	This study	NS320
S. Typhimurium, IR715 Δ*gltA*Δ*aspC*Δ*phoN*::Km^R	This study	NS321
Plasmid	**Source**	**Identification**
Plasmid: pKD46, Spec^R P_{BAD}-*gam-beta-exo oriR101 repA101*^{ts}	Datsenko and Wanner[54]	pKD46
Plasmid: pKD3, Carb^R FRT Cm^R FRT PS1 PS2 *oriR6Kγ*	Datsenko and Wanne[54]	pKD3
Plasmid: pKD13, Carb^R FRT Km^R FRT PS1 PS4 *oriR6Kγ*	Datsenko and Wanner[54]	pKD13
Plasmid: pCP20, CarbR FLP *oripSC101* CmR r*epA101*^{ts} MbeC	Datsenko and Wanner[54]	pCP20

588

589

590 **Supplementary Table 2: Primers used in this study.**

Primer	Sequence
IR715_gltA_delF	GCT ATT GAA CTG GAT GTG CTA AAA GGT ACA CTC GGT CAA TG TAG GCT GGA GCT GCT TCG
IR715_gltA_delR	GAT TTT CAT GCC GTC AGT GTG CAT TTC ATT CCA GTG TGC AT TCC GGG GAT CCG TCG ACC
IR715_gltA_conF	GGT CAC TCT TTC ACC TGT TA
IR715_gltA_conR	GCC GGA AGG TGC AGA TAG AG
IR715-sdhA-del-F1	CAA ACC TGT GCG CTG CTC TCG AAA GTC TTC CCG ACC CGT T TG TAG GCT GGA GCT GCT TCG
IR715-sdhA-del-R1	CTG ATA CAG GGT ATG ACA CAA CCA GTT GGC ATC ATC ACG CAT TCC GGG GAT CCG TCG ACC
IR715-sdhA-con-F1	GCA ACG CCT CCG CAT TAG GA
IR715-sdhA-con-R1	CAC ACC TTC GCG GCA GGA AC
aspC-del-F1	ATA GCG GAT TTC CCT TCT GTA ACT ATA ATG GAA CCT CGT CTG TAG GCT GGA GCT GCT TCG
aspC-del-R1	ATT GCA GGC TTT TTT ATC GGT CAC GCC AGT CGG CAG CTT TAT TCC GGG GAT CCG TCG ACC
aspC-con-F1	TAC TTA CCA GTT CTG ATC AGC
aspC-con-R1	CGC TTG GCG ATG ATG TGA C
thrA_qFwd	GGCGTTCTACAGCCACTATTATC
thrA_qRev	CCGTAACAGATCGGCAAACA
metL_qFwd	GGGCGTTACTGGCTGTATAA
melL_qRev	CGCTGATCGAGAGAATCGTATC
lysC_qFwd	GGTACGCTGGTGTGCAATAA
lysC_qREv	CCTCGTGAGTGCAGCATATT
pyrI_qFwd	AACCAGTATCCTCCAGCTTTG
pyrI_qRev	TTGGCCAGCACCACATAAT
pyrB_qFwd	CAGCCGCGACGATCTTAAT
pyrB_qRev	GCTGGCGATCACTTTATGTTTC
asnA_qFwd	GAGGCTATATGGGCAGGAATTA
asnA_qRev	CAGTTCCTGACTGTGAACAAAC
IR715_qPCR_aspA_F	TCGTAACGGTGGTGTCGTTA
IR715_qPCR_aspA_R	CTGTGGCGCATATGTTATGG
IR715_qPCR_aspC_F	CAGACCGCTGAATGAGAACA
IR715_qPCR_aspC_R	GCCATTCGCGCTAACTACTC
IR715_qPCR_dcuA_F	GATGACCCTGGATGACGCTA
IR715_qPCR_dcuA_R	AAACCGCTGATGAACACCAC
K1	CAGTCATAGCCGAATAGCCT

591

592

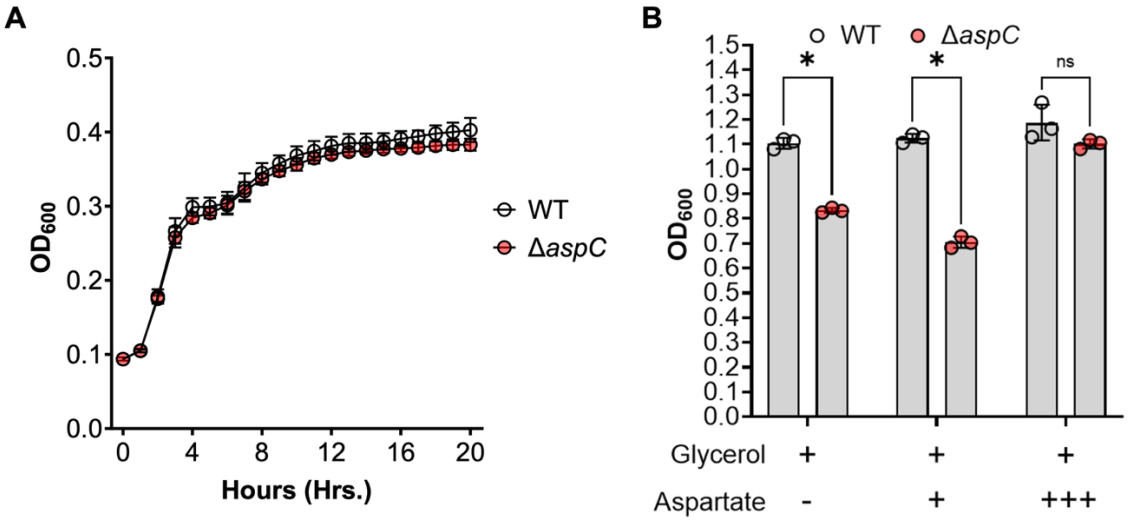

593
594
595 **Figure S1: Deletion of Δ*aspC* does not confer a growth defect compared to WT when cultured**
596 **anaerobically in LB broth but does under hypoxia in minimal media.** Related to Figure 4. Growth of WT and
597 *aspC* deficient *S*. Tm (A) anaerobically in LB or (B) under hypoxic (0.8% O_2) NCE minimal media supplemented
598 with Glycerol and (+) 0.1mM or (+++) 10mM Aspartate with Glycerol.N=3 per condition, Geometric mean and
599 Geometric SD Multiple t-test, P=*,<0.05.
600

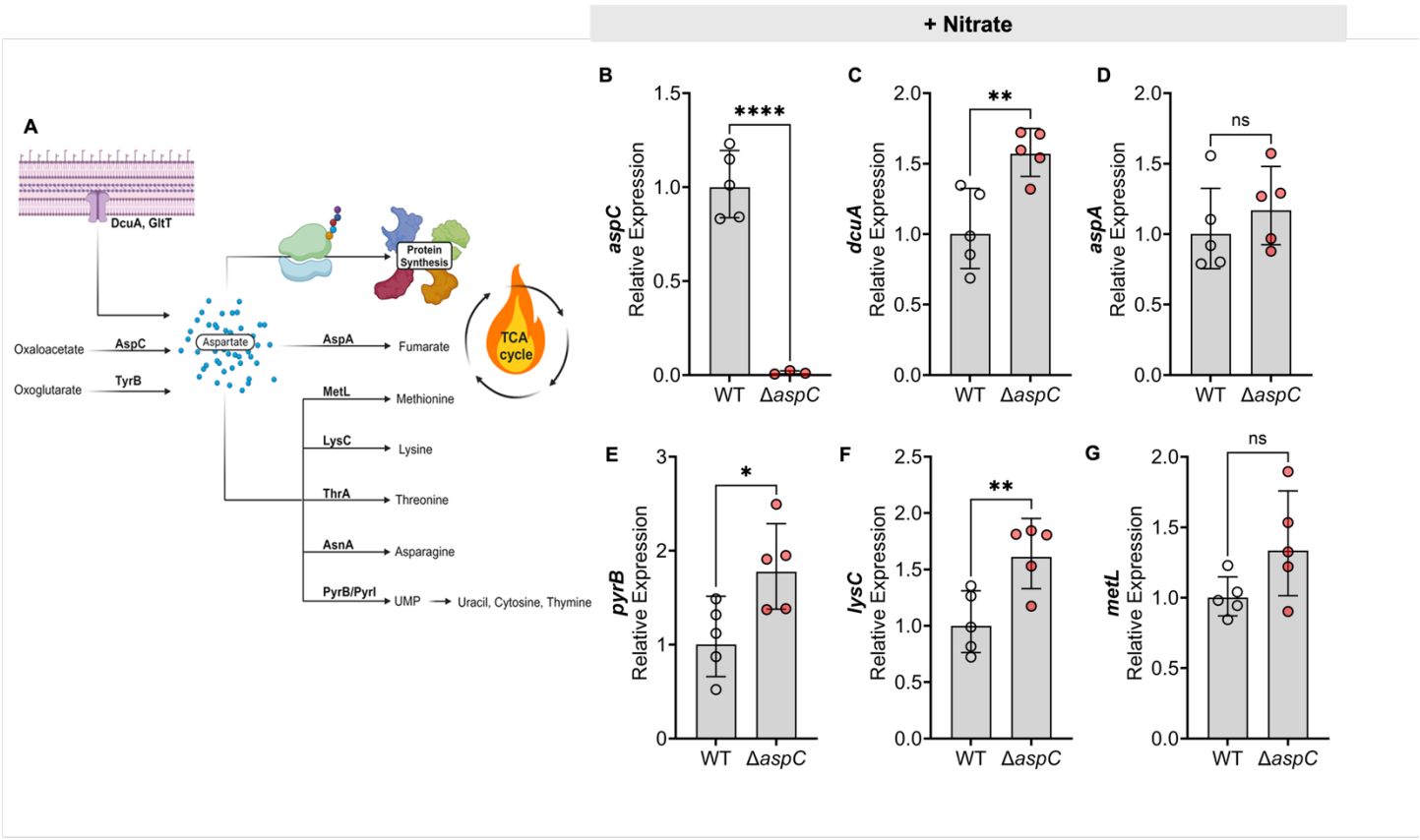

Figure S2: AspC-deficiency alter central metabolism of *S.* Tm during anaerobic nitrate respiration. Related to Figure 5. Aspartate can fuel several other metabolic processes, we investigated the expression of genes involved in aspartate utilization in conditions supplemented with Nitrate, in which we observe a significant growth and fitness defect of the *aspC*-deficient *S.* Tm compared to the WT. (A) Schematic for the central role of aspartate in *S.* Tm metabolism. (B-G) Gene expression of WT and Δ*aspC* grown under nitrate respiration with glycerol as the sole-carbon source. (B) *aspC,* (C) *dcuA,* (D) *aspA,* (E) *pyrB*, (F) *lysC*, (G) *metL* N=5 per condition, Geometric mean and Geometric SD, Unpaired t-test; P=*, <0.05; **,<0.01; ***, <0.001; ****, <0.0001

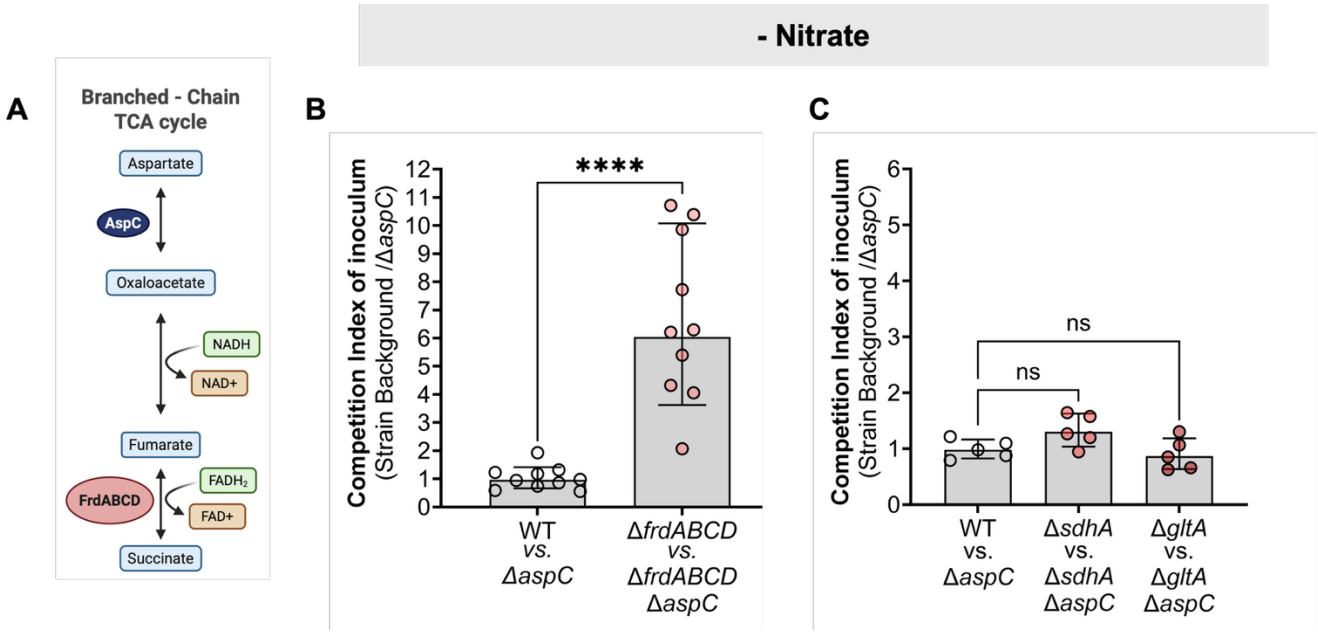

Figure S3: Deletion of *frdABCD* but not *sdhA* or *gltA,* significantly increases fitness defect of *aspC*-deficient *S.* Tm during growth in mucin media alone. Related to Figure 5. (A) Competitive index of inoculum for loss of *aspC* in WT and *frdABCD*–deficient *S*. Tm backgrounds in the absence of Nitrate**.** (B) Competitive index of inoculum for loss of *aspC* in WT and *gltA or sdhA*–deficient backgrounds in the absence of Nitrate**.** N=10 per condition, Geometric mean and Geometric SD. Unpaired t-test, P=****, <0.0001.